



Advanced Composite Materials

Publication details, including instructions for authors and subscription information:

<http://www.tandfonline.com/loi/tacm20>

Characteristics of Expanded Graphite Filled Conductive Polymer Composites for PEM Fuel Cell Bipolar Plates

K. S. Oh^a, S. I. Heo^b, J. C. Yun^c, Y. C. Yang^d & K. S. Han^e

^a Department of Mechanical Engineering, Pohang University of Science and Technology, San 31 Hyoja-dong, Nam-gu, Pohang, 790-784, Korea

^b Department of Mechanical Engineering, Pohang University of Science and Technology, San 31 Hyoja-dong, Nam-gu, Pohang, 790-784, Korea

^c Department of Mechanical Engineering, Pohang University of Science and Technology, San 31 Hyoja-dong, Nam-gu, Pohang, 790-784, Korea

^d Fuel Cell Vehicle Team, Advanced Technology Center, Research & Development Division for Hyundai Motor Company & Kia Motors Corporation, 104, Mabuk-dong, Giheung-Gu, Yongin, 446-912, Korea

^e Department of Mechanical Engineering, Pohang University of Science and Technology, San 31 Hyoja-dong, Nam-gu, Pohang, 790-784, Korea; Email: kshan@postech.ac.kr

Version of record first published: 02 Apr 2012.

To cite this article: K. S. Oh, S. I. Heo, J. C. Yun, Y. C. Yang & K. S. Han (2008): Characteristics of Expanded Graphite Filled Conductive Polymer Composites for PEM Fuel Cell Bipolar Plates, *Advanced Composite Materials*, 17:3, 259-275

To link to this article: <http://dx.doi.org/10.1163/156855108X345261>

PLEASE SCROLL DOWN FOR ARTICLE

Full terms and conditions of use: <http://www.tandfonline.com/page/terms-and-conditions>

This article may be used for research, teaching, and private study purposes. Any substantial or systematic reproduction, redistribution, reselling, loan, sub-licensing, systematic supply, or distribution in any form to anyone is expressly forbidden.

The publisher does not give any warranty express or implied or make any representation that the contents will be complete or accurate or up to date. The accuracy of any instructions, formulae, and drug doses should be independently verified with primary sources. The publisher shall not be liable for any loss, actions, claims, proceedings, demand, or costs or damages whatsoever or howsoever caused arising directly or indirectly in connection with or arising out of the use of this material.

Characteristics of Expanded Graphite Filled Conductive Polymer Composites for PEM Fuel Cell Bipolar Plates

K. S. Oh^a, S. I. Heo^a, J. C. Yun^a, Y. C. Yang^b and K. S. Han^{a,*}

^a Department of Mechanical Engineering, Pohang University of Science and Technology,
San 31 Hyoja-dong, Nam-gu, Pohang, 790-784, Korea

^b Fuel Cell Vehicle Team, Advanced Technology Center, Research & Development Division for
Hyundai Motor Company & Kia Motors Corporation, 104, Mabuk-dong, Giheung-Gu,
Yongin, 446-912, Korea

Received 12 November 2007; accepted 20 December 2007

Abstract

This study aims to optimize the mechanical and electrical properties of electrically conductive polymer composites (CPCs) for use as a material of bipolar plates for PEM fuel cells. The thin CPCs consisting of conductive fillers and polymer resin were fabricated by a preform molding technique. Expanded graphite (EG), flake-type graphite (FG) and carbon fiber (CF) were used as conductive fillers. This study tested two types of CPCs, EG/FG filled CPCs and EG/CF filled CPCs, to optimize the material properties. First, the characteristics of EG/FG filled CPCs were investigated according to the FG ratio for 7 and 100 μm sized FG. CPCs using 100 μm FG showed optimal material properties at 60 wt% FG ratio, which were an electrical conductivity of 390 S/cm and flexural strength of 51 MPa. The particle size was an important parameter to change the mechanical and electrical behaviors. The flexural strength was sensitive to the particle size due to the different levels of densification. The electrical conductivity also showed size-dependent behavior because of the different contributions to the conductive network. Meanwhile, the material properties of EG/CF filled CPCs was also optimized according to the CF ratio, and the optimized electrical conductivity and flexural strength were 290 S/cm and 58 MPa, respectively. The electrical conductivity of this case decreased similarly to the EG/FG filled case. On the other hand, the behavior of the flexural strength was more complicated than the EG/FG filled case, and the reason was attributed to the interaction between the strengthening effect of CF and the deterioration of voids.

© Koninklijke Brill NV, Leiden, 2008

Keywords

Conductive polymer composites (CPCs), expanded graphite (EG), electrical conductivity, flexural strength

* To whom correspondence should be addressed. E-mail: kshan@postech.ac.kr
Edited by KSCM

1. Introduction

The fuel cell is a relatively new but fast developing power system that is sustainable, clean and environmental friendly. There are several types of fuel cells of commercial importance: alkaline, DMFC, MCFC, PAFC, PEMFC, SOFC, etc. [1–3]. Recently, polymer electrolyte membrane fuel cells (PEMFC) have been explored as the most promising power sources for various portable electronic devices and transportation applications. They offer the advantages of low operating temperature, compactness, light weight, high power density and energy conversion efficiency [4–6].

A key component of the fuel cell stack is the bipolar plates that account for 80% of the total weight and 45% of the stack cost [7, 8]. The functions of the bipolar plates in the stack are to distribute the fuel and oxidant within the cell, separate the individual cells in the stack, carry current along the cells and carry water away from each cell. With the bipolar plate accounting for the bulk of the stack, it is desirable to fabricate bipolar plates that are as thin and lightweight as possible. Therefore, the bipolar plates have to have a high electrical conductivity, sufficient flexural strength, etc. [9, 10]. There are many kinds of materials used for the bipolar plates, such as machined graphite plates, metal sheets, graphite composites, etc. The most commonly used material has been machined graphite plates with micro-channels made by direct machining on the resin-infiltrated plates. But the expensive cost for machining all the channels has blocked their commercialization. Metal plates such as titanium and stainless steel offer low thickness and weight, excellent electrical and thermal properties, and good mechanical and gas permeation characteristics, but have several problems such as spring backs and corrosion [11, 12]. The conductive polymer composite (CPC) is a powerful candidate for the bipolar plates because it is light in weight and can be molded into any shape and size, and also provides a low manufacturing cost, high electrical conductivity and good electrochemical stability [13]. However, the fabrication of the thin-type bipolar plates for a PEMFC has the following issues associated with high conductive-filler loadings: substantial reductions in the mechanical properties and ductility [14]. Also, research to achieve high electrical conductivity at low filler loadings has been attempted by using liquid crystal polymers, which have a high glass transition temperature and good mechanical properties due to their molecular structure [15].

A number of manufacturers and governments have supported ongoing research about the optimization of composite bipolar plates to maintain both the high electrical conductivity and good mechanical properties. These works have been carried out with respect to the size, shape and weight contents of fillers, etc. [16–19]. Many researchers have focused on the commercialization of PEM fuel cells, especially the reduction of the cost and weight of the bipolar plates [20, 21]. The compression molding method has already proven to be a good method to fabricate fuel cell bipolar plates to ensure superior material properties, but the curing time (longer than 10 min) was a considerable barrier to its cost-benefit production [14].

Lately, composite bipolar plates with graphite loadings above 80 wt% have been produced by injection molding to satisfy the U.S. D.O.E.'s specification of an electrical conductivity of 100 S/cm or above [22, 23]. However, large thin plates comparable to existing machined graphite plates cannot easily be manufactured using injection molding. Thus, another method, such as wet-lay composites, is needed to improve manufacturing productivity [24, 25]. A preform molding technique consisting of pre-curing and stamping steps was developed in our laboratory to reduce the high-pressure compression time to less than 3 min, and the pre-curing and stamping conditions were optimized based on the formability and the material properties of CPCs [26].

This study is focused on the optimization of mechanical and electrical properties of EG filled hybrid CPCs prepared by a preform molding technique. The conductive fillers used were expanded graphite (EG), flake-type graphite (FG) and carbon fiber (CF), and the experiments were carried out for three cases of CPCs using 100 μm FG, 7 μm FG and CF. The effect of weight composition on the mechanical and electrical properties of three composite plates were investigated.

2. Experimental

2.1. Materials

Conductive polymer composites (CPCs) are combinations of at least two materials in which one of the materials, called the conductive filler, is in the form of fibers or particles, and embedded in the other materials called the polymer resin. The novolak-type phenol powder (Kolon Chemical, Korea) was selected as a thermosetting polymer resin. This resin had been widely used in various industrial fields because it had a lot of advantages, such as a low shrinkage rate, good chemical stability, high thermal resistance and mechanical strength [27]. The conductive fillers used in this study were expanded graphite (EG), flake-type graphite (FG) and carbon fiber (CF). Table 1 shows the target functions of the fillers and their contributions to the material properties. The characteristics of raw materials are specified in Table 2, where the density of EG is an innate density measured under no compaction.

Table 1.

The target functions of fillers and their contributions to material properties

			Contribution to material properties	
			Electrical conductivity	Flexural strength
Filler	EG	Formability	H	L
	FG	Densification	M	M
	CF	Strengthening	L	H

Contribution level: H-high, M-middle and L-low.

Table 2.
Characteristics of used materials

	Type	Diameter (μm)	Length (μm)	Density (g/cm ³)
Filler	EG	500	5000	0.015
	FG	100	–	2.2
		7	–	2.2
	CF	18	200	2.0
Resin	Phenol powder	25	–	1.07

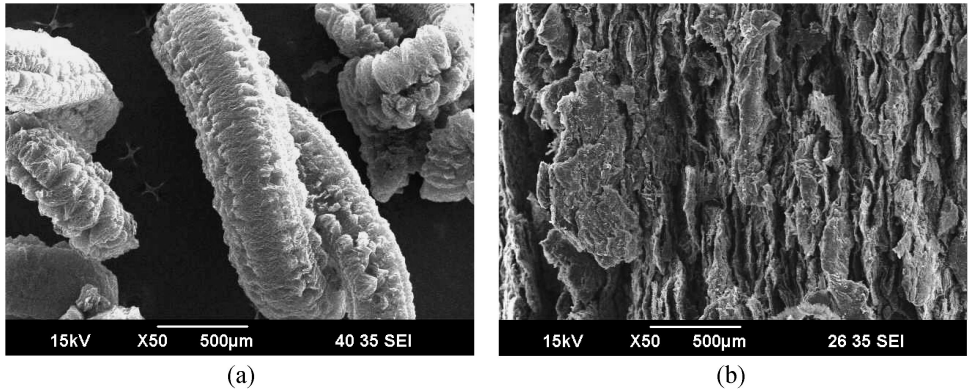


Figure 1. Shape of EG: (a) raw state; (b) horizontally compressed state at 7 MPa.

Figure 1(a) and 1(b) shows the shapes of a raw EG and compressed EG, respectively. Industrial production of EG is usually derived from graphite intercalation compounds (GIC) which were prepared by treating graphite flakes with sulphuric acid and a strong oxidizing agent. By submitting these sulphuric acid-based GIC precursors to a brutal thermal shock, the sudden volatilization of the intercalation induces a huge unidirectional expansion of the initial graphite plates [28]. At the beginning of the compaction of the loose packed EG, the worm-like particles rearrange spatially, and then the rigidity threshold is met as the EG undergoes compaction [29]. After that threshold, more compaction kept on reducing the intra-voids of EGs, which finally returned to a shape similar to the original graphite flake, while the surface of those was highly porous and flat-wide. The raw EGs were beneficial to fabricate a preform at a low pressure because they could bind the fillers by utilizing their tangled structure, and the compressed EGs were excellent in forming a conductive network in CPCs owing to wide direct contact areas between them. From those reasons, EGs were the most suitable filler for both curing steps of the preform molding technique. However, the compressed EGs were so porous and flexible that it was hard to guarantee a good physical densification and high mechanical strength of EG-filled CPCs.

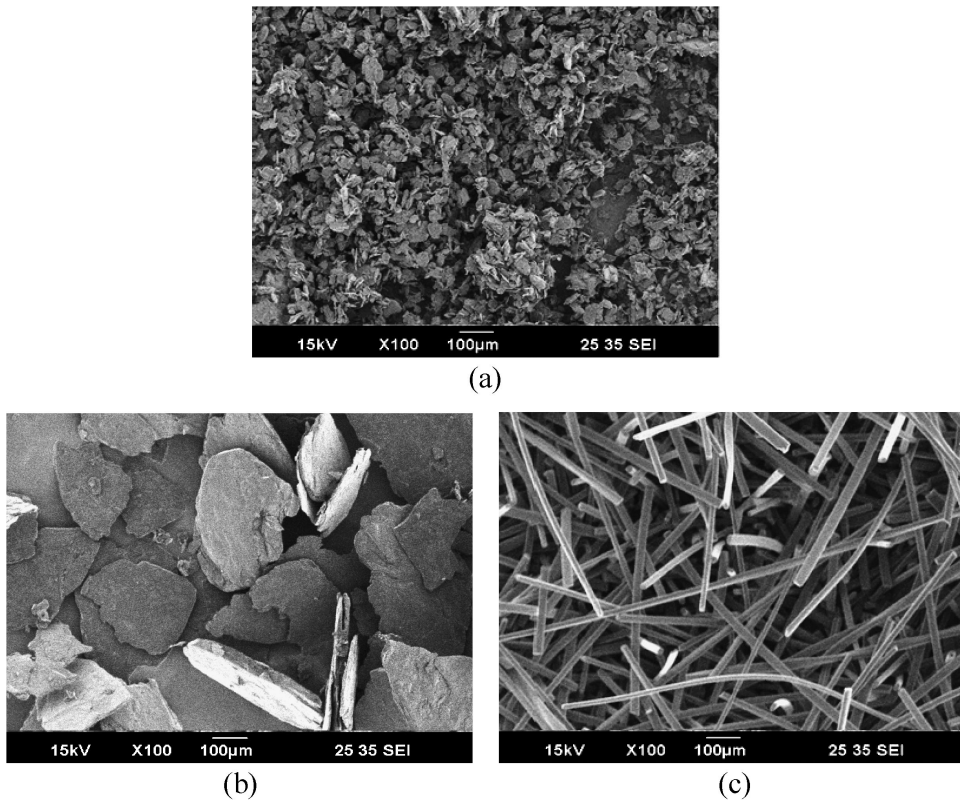


Figure 2. Shape of ancillary filler: (a) 7 μm FGs; (b) 100 μm FGs; (c) CFs.

FG and CF were separately added to the EG-filled CPCs for the purpose of enhancing the level of densification and the mechanical strength of CPCs. Figure 2 shows the shapes of FG and CF. FG particles were suitable for the filler of CPCs because of their good electrical conductivity, mechanical strength and immunity to corrosion [30]. The diameters of FG particles used in this study were 7 and 100 μm , and their thicknesses were several microns. The analysis of particle size distributions of each FG were carried out using a Laser Particle Size Analyzer (CILAS 920 Liquid, CILAS, France) and the size distributions are shown in Fig. 3. CF was also a well-known reinforcement which had been widely used for a long time and also has good characteristics like those of FG. On account of these characteristics, FG and CF were selected as ancillary fillers of CPCs. These graphite particles were supplied by Hyundai-kish, Korea and CF was provided by KRECA, Japan.

2.2. Fabrication

Both EG/FG filled CPCs and EG/CF filled CPCs were fabricated by a preform molding technique, which was developed at our laboratory [26]. The fabrication process of this technique consisted of material mixing, precuring and stamping. Conductive fillers and phenol resin were mechanically mixed at the test ratio and

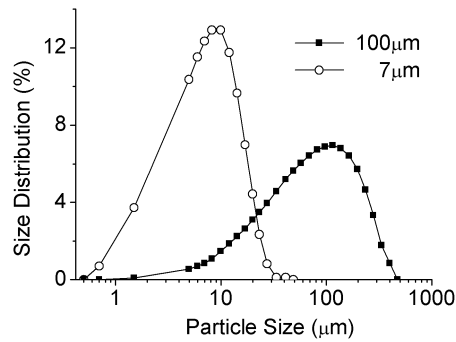


Figure 3. Size distribution of 7 μm and 100 μm FGs.

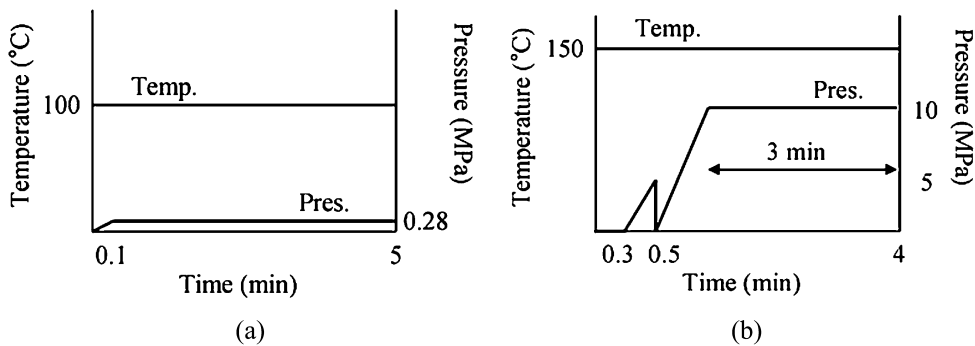


Figure 4. Curing cycle of preform molding technique [26]: (a) precuring; (b) stamping.

shaken for approximately 30 min to make a uniform blend of the materials. This blend was poured into the precuring mold at room temperature. The precuring mold was placed on a preheated plate of the hot press (Tetrahedron 40 ton, US) at 100°C , slightly higher than the melting point of phenol powder (90°C). Precuring step was carried out at 100°C , 0.3 MPa for 5 min. The preform made in the precuring step was inserted into the stamping mold at 150°C and preheated for 30 s to soften the precured phenol resin. After preheating, the preform within the steel stamping mold was compressed to 10 MPa at 150°C and maintained for just 3 min. This high compression caused the re-melted phenol resin to infiltrate into the voids of the preform. Figure 4(a) and 4(b) represents the precuring and stamping cycles, respectively [26].

However, the EG/FG filled CPCs with 0:75:25 wt% (EG/FG/resin) composition were prepared by a pre-existing compression molding method because it was very hard to get a well-made preform without any addition of EGs. In this case, molds had to be cooled down to room temperature before dispersion of the blend to prevent the mixed blend from curing. Figure 5 represents the curing cycle of the existing compression molding method [18].

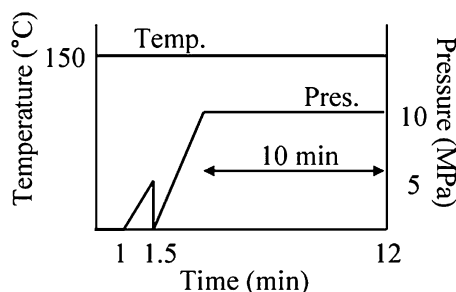


Figure 5. Curing cycle of compression molding method [18].

2.3. Measurements

The analyses of microstructures and relative densities were performed to examine the manufactured state and estimate the amount of voids in the CPC specimens. The microstructures of specimens were observed with a Philips XL30S Scanning Electron Microscope, and the relative densities were represented by a non-dimensional ratio of the physical density to the theoretical density. The physical density of the tested specimen was measured based on Archimedes's principle (ASTM D792-00) and the theoretical density was calculated by the linear summation of the innate densities of the component materials. The innate densities of FG, CF and phenol powder did not vary even though they were under various compaction pressures. The density of an uncompressed EG, however, was initially 0.015 g/cm^3 , and then increased up to nearly 2.0 g/cm^3 with the increase of the compaction pressure due to the reduction of inter-particle and intra-particle voids. At the beginning of the compaction of the loose packed EG, the worm-like EGs rearrange spatially, and then the rigidity threshold is met as the EG undergoes compaction [26]. After this threshold, the constant ratio of intra-particle void to total void and the density of EG at a given pressure are calculated according to the following equations [28]:

$$\text{constant } A = \frac{1 - \frac{\text{density of the compressed material}}{\text{density of the EG}}}{1 - \frac{\text{density of the compressed material}}{\text{density of graphite}}} \quad (1)$$

$$\text{density of EG} = \frac{\text{density of compressed material}}{1 - A \times \text{overall porosity}} \quad (2)$$

The constant A of EG used in this study was experimentally derived as 0.33 by the normal compaction test, and finally the density of EG was calculated at 1.822 g/cm^3 .

The electrical conductivity (in-plane) was measured by the four-point probe technique. The samples were cut to a size of $80 \times 12.7 \times 2.4 \text{ mm}^3$ using a bandsaw. A current was applied stepwise through the two outermost probes and the result

voltage across the two inner probes was measured by a multimeter 34491A (Agilent). The electrical conductivity is calculated according to the following equation:

$$\sigma = \frac{I}{V} \cdot \frac{L}{A}, \quad (3)$$

where I is the applied current, V is the resultant voltage potential, A is the cross-sectional area of the specimen and L is the distance between the inner probes.

The flexural strength was measured by the three-point bending test in accordance with ASTM D790-02 using a universal testing machine (Shimadzu 5 ton, Japan). Specimens used in measuring the electrical conductivity were reused in this test for consistency of experiments. The support span to depth ratio (L/t) was 16, and the cross-head speed was 1 mm/min. The flexural strength was calculated according to the following equation:

$$\text{Flexural strength} = \frac{3PL}{2Wt^2}, \quad (4)$$

where P is the breaking force of the specimen, L is the support span, W is the width of the specimen and t is the thickness of the specimen.

3. Results and Discussion

3.1. Analysis of EG/FG filled CPCs

The principal variables affecting the mechanical and electrical properties of EG/FG filled CPCs were the weight ratio and the particle size of FG. It was decided to fix the weight ratio of the phenol resin at 25 wt% in accordance with the previous study [26]. The remainder, 75 wt%, was allocated for conductive fillers divided into various ratios of EG and FG. The experimental range of FG ratio was 0 and 37.5–75 wt% for both cases of CPCs using 7 and 100 μm FGs. At 0 wt% FGs, the conductive filler was only EG. The experiments in the range lower than 37.5 wt% were excluded due to insufficient mechanical strengthening. At 75 wt% FGs, there was no EG in the CPCs.

3.1.1. Relative Density

To verify the level of a densification of EG/FG filled CPCs, the relative density was investigated according to the weight ratio and the particle size of FG. The relative density is inversely proportional to the amount of pores in CPCs, and is hence directly related to the level of a densification. Because EG was a highly porous material, the amount of pores should be verified considering the intra-particle pores of EGs and inter-particle pores between the fillers. In this study, the compaction pressure was sufficiently high (almost 10 MPa) that the amount of the inter-particle pores could be regarded as being similar for both CPCs using 7 and 100 μm FGs. Therefore, the level of a densification of CPCs could be determined by the amount of the intra-particle pores only.

Figure 6 represents the behavior of the relative density according to the weight ratio and particle size of FG. The relative density was initially about 0.8 at the FG

ratio of 0 wt%. As the FG ratio increased from 37.5 to 75 wt%, the relative density kept on increasing up to the value of 0.97–0.98, which could be considered quite a high level of densification. This tendency resulted from the reduction of absolute amounts of EGs, which was directly proportional to the decrease of the amount of the intra-particle pores.

The increasing behavior, however, showed a different aspect according to the particle size of FG. At FG ratios lower than 70 wt%, the relative density was comparatively higher in the case using 100 μm FG than 7 μm FG. The difference of the relative density could be verified by considering the amounts of the intra-particle pores of each CPC. Figure 7 showed the microstructures of fractured surfaces for specimens of CPCs using 7 and 100 μm FGs under the same FG ratio of 67.5 wt%. As shown in Fig. 7(a), 100 μm FG particles and compressed EGs formed a stack structure in which EGs were sufficiently compacted. On the other hand, Fig. 7(b) showed that 7 μm FG particles were randomly located between compressed EGs, so the compaction of EGs was not enough. This difference of the compaction brought

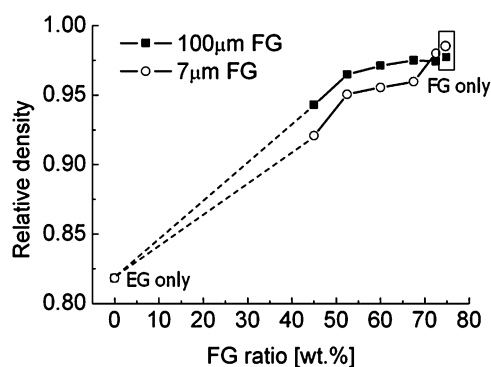


Figure 6. Relative density of EG/FG filled CPCs according to weight ratio and particle size of FG.

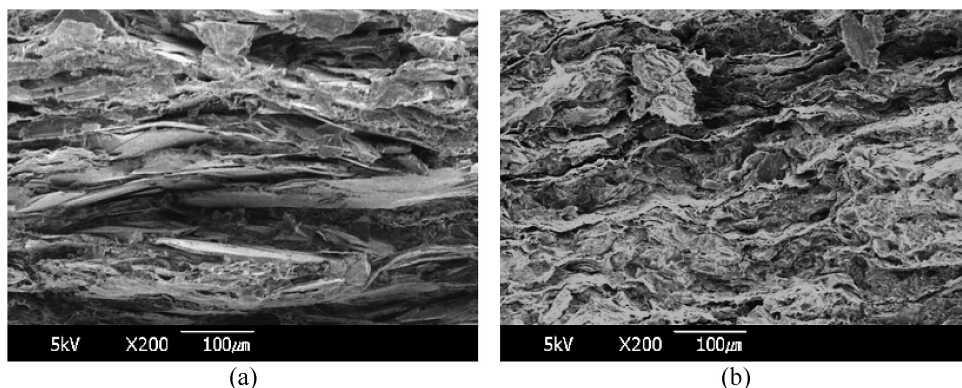


Figure 7. Microstructure of fractured surface of CPCs at FG ratio of 67.5 wt%: (a) 100 μm FG and (b) 7 μm FG.

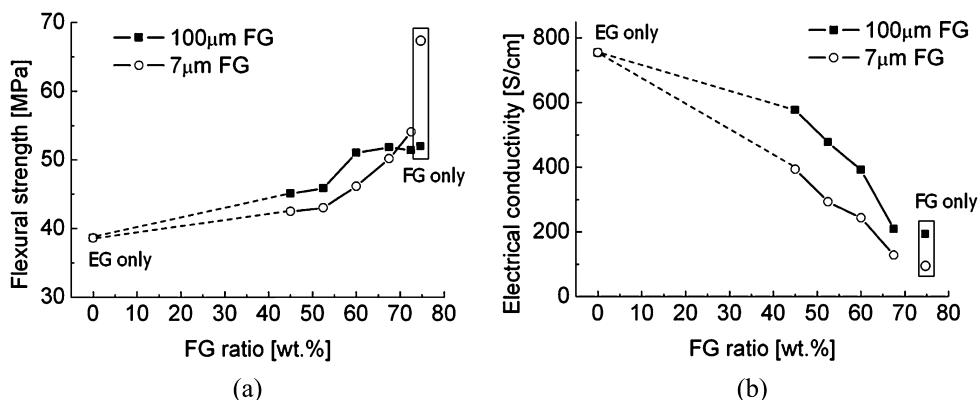


Figure 8. Material properties of EG/FG filled CPCs according to weight ratio and particle size of FG: (a) flexural strength and (b) electrical conductivity.

on the relative difference in the level of a densification. At FG ratios greater than 70 wt%, the EG ratio was very low, so the role of EGs was confined to prevent the preform from breaking and had an insignificant influence on material properties. Then, the relative densities of EG/FG filled CPCs were similar to those of FG-only filled CPCs; that is, the relative densities of both cases become similar or slightly higher in CPCs using 7 μm FG.

3.1.2. Flexural Strength

The bipolar plates should have adequate mechanical properties to bear the loads in fuel cell stacks. However, CPCs with high filler loadings had difficulty reaching a high electrical conductivity and sufficient mechanical properties. Therefore, the experiments with respect to the various FG ratios were carried out to optimize the mechanical properties (such as flexural strengths).

As shown in Fig. 8(a), the behavior of the flexural strength according to the weight ratio and particle size of FG was similar to that of the relative density. The flexural strengths of both CPCs kept on increasing as the FG ratio increased, and the increasing behavior was different according to the particle size of FG. The pores in CPCs generally resulted in stress concentrations that lowered the flexural strength, so the behavior of flexural strength could be explained by considering the level of densification, or relative density of CPCs.

The flexural strength of CPCs using 100 μm FG rapidly increased up to 51 MPa until around 60 wt% FG and scarcely changed above that ratio. This result indicates that the densification of CPCs using 100 μm FG attained a sufficient level and that little further densification occurred when the FG ratio was increased further. On the other hand, the flexural strength of CPCs using 7 μm FG was about 43 MPa at 60 wt% FG, which indicates the insufficient densification of CPCs. As the FG ratio increased, however, the flexural strength was further increased and reached over 68 MPa because of the increasing densification of CPCs. Finally, the flexural strength of CPCs using 7 μm FG surpassed that of CPCs using 100 μm FG. These

behaviors were supported by the microstructure analysis of polished side surfaces of tested specimens.

Figure 9(a) and 9(b) represents the SEM images of CPCs using 100 μm FG at FG ratio of 67.5 and 75 wt%, respectively. In the case of 67.5 wt%, EGs and FG particles (dark gray) formed the stack structure mentioned in the relative density section, so the compaction of EGs was sufficient. That is, the microstructure of this case was similar to that of the case of 75 wt% in Fig. 9(b). This fact indicated that no further compaction occurred even though the FG ratio increased, and the flexural strength was maintained above the FG ratio of 60 wt%, at which the densification was sufficiently achieved. On the other hand, the SEM images of CPCs using 7 μm FG at FG ratios of 67.5 and 75 wt% showed different microstructures, as shown in Fig. 10. Insufficiently compacted EGs existed in the 67.5 wt% CPC in Fig. 10(a), meaning that the densification was not sufficient. That is, the microstructure at this FG ratio was different from that of the case of 75 wt% in Fig. 10(b), which had a

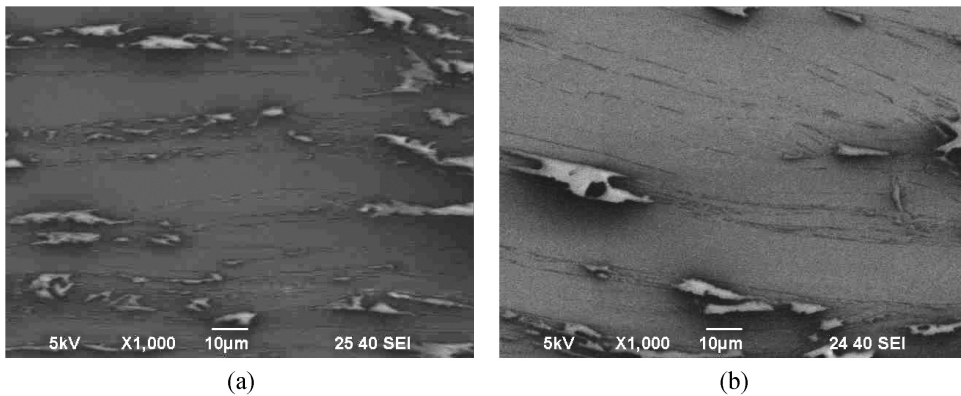


Figure 9. Microstructure of polished surface of CPCs using 100 μm FG: (a) 67.5 wt% and (b) 75 wt%.

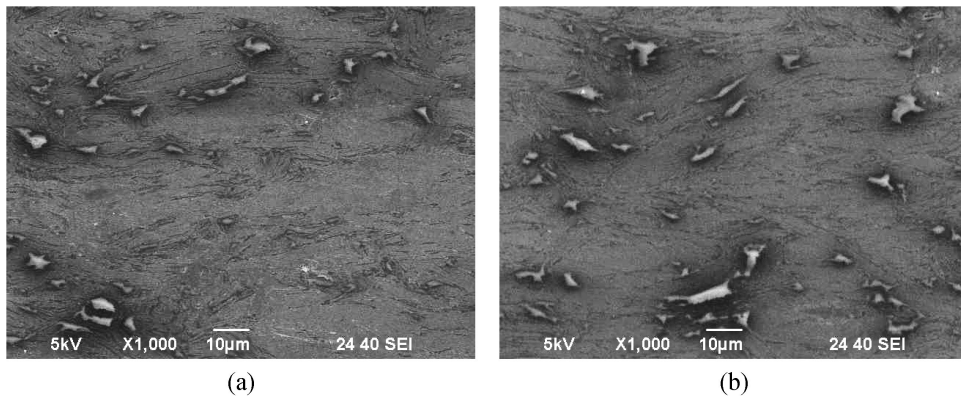


Figure 10. Microstructure of polished surface of CPCs using 7 μm FG: (a) 67.5 wt% and (b) 75 wt%.

stack structure. Therefore, as the FG ratio increased, further compaction occurred, so the flexural strength increased continuously until the FG ratio of 75 wt%.

3.1.3. *Electrical Conductivity*

The bulk electrical conductivity along the in-plane direction is one of the most important properties of fuel cell bipolar plates. The prepared specimens of EG/FG filled CPCs all have high electrical conductivity regardless of the FG ratio, as shown in Fig. 8(b), with all values exceeding the commercial requirements (>100 S/cm) for composite bipolar plates. It is well known that the electrical conductivity of CPCs is closely related to the formation of a conductive network among the conductive fillers. In general, the flat surface of a compressed EG particle was relatively longer and wider than that of a FG particle, so EG has an advantage in forming a conductive network in EG/FG filled CPCs. Even though FG particles are also conductive, their contribution to the electrical conductivity was much lower.

As shown in Fig. 8(b), the electrical conductivity decreased with the increase of the FG ratio in both cases. As previously mentioned, this tendency resulted from the reduction of the amount of EG, which is excellent in forming a conductive networking. Figure 8(b) also indicates that the decreasing tendency of the electrical conductivity was apparently more obvious for 7 μm FG than for 100 μm FG. This result was attributed to the difference in the electrical contribution with respect to the size of FG particle. The contact area between fillers was larger in the case using the larger FG particles, so the electrical contribution to the conductive network was superior.

3.2. *Analysis of EG/CF filled CPCs*

Several kinds of fibers have been widely used as reinforcements in variously aimed composites. In this study, CF was selected for the ancillary filler with the object of strengthening the mechanical properties of EG filled CPCs. The effect of CF weight ratio on the mechanical and electrical properties was investigated experimentally to find the optimal properties satisfying the commercial targets of fuel cell bipolar plates. The weight ratio of phenol resin was fixed at 40 wt%, the ratio from an experiment similar to our previous study [26]. The remainder, 60 wt%, was allocated for conductive fillers divided into the ratios of EG and CF. The experimental range of CF ratio was 6–42 wt%. The experiments in the range lower than 6 wt% and greater than 42 wt% were excluded; the former due to the insufficiency of mechanical strengthening, and the latter because of the occurrence of voids among the abundant fibers which made it hard to get well-made specimens.

3.2.1. *Relative Density*

As discussed in the analysis of EG/FG filled CPCs, the relative density was involved with the level of a densification. Figure 11(a) gives the behavior of the relative density according to the CF ratio.

The relative density was initially about 0.97 at the CF ratio of 6 wt%, and then decreased only slightly until 24 wt%. As the CF ratio further increased, however,

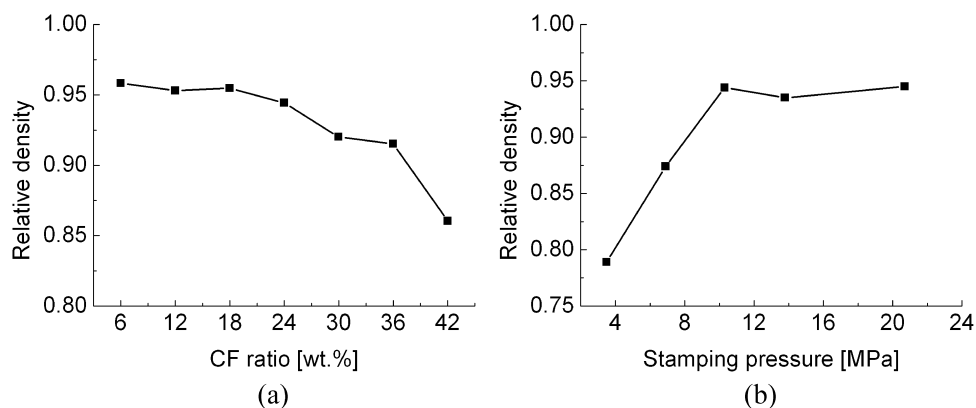


Figure 11. Relative density of EG/CF filled CPCs: (a) according to CF ratio and (b) according to stamping pressure (CF ratio of 24 wt%).

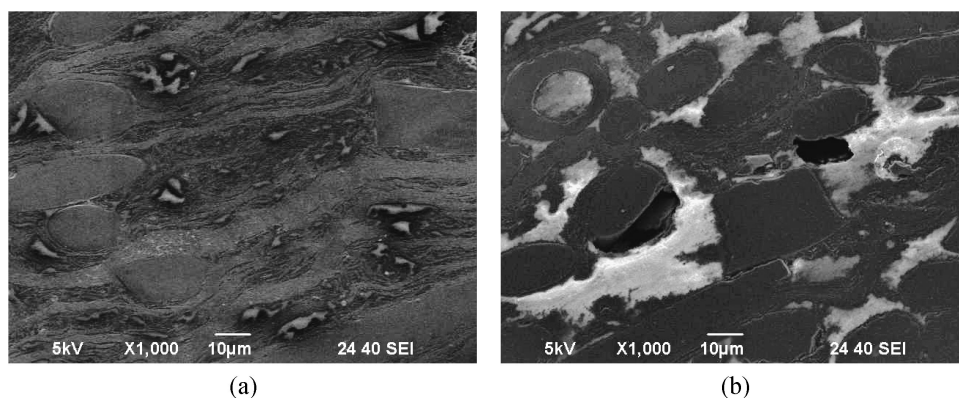


Figure 12. Microstructure of polished surface of EG/CF filled CPCs: (a) 24 wt% and (b) 36 wt%.

the relative density decreased sharply. The reason for the latter decreasing tendency could be the occurrence of voids which were generated among the excess fibers, which would cause a falling-off in the densification of CPCs. Figure 12(b) shows the appearance of voids according to the increase of the fiber ratio. Meanwhile, it was reported that the level of densification of CF-containing hybrid CPCs could be upgraded by the increase of the stamping pressure [31]. This means that an insufficient stamping pressure could be a possible reason for the occurrence of the voids and drop of material properties, but a test with respect to the stamping pressure, as shown in Fig. 11(b), indicated that the relative density was not improved even though the stamping pressure was increased over 20 MPa. Thus, the stamping pressure of 10 MPa was enough to fabricate EG/CF filled CPCs, which implies that the decrease of material properties was dependent on the CF ratio, not the stamping pressure. The occurrence of voids will be a considerable barrier to the manufactura-

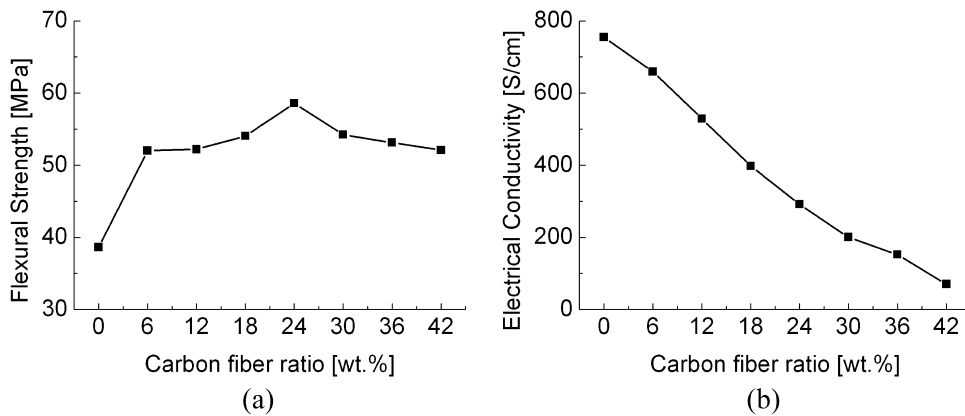


Figure 13. Material properties of EG/CF filled CPCs according to weight ratio of CF: (a) flexural strength and (b) electrical conductivity.

bility of composite bipolar plates, so a manufacturing method that does not generate voids should be developed in future works.

3.2.2. Flexural Strength

CFs have been used to enhance the mechanical properties of EG filled CPCs. As shown in Fig. 13(a), all tested CPCs show sufficiently high flexural strengths of greater than 50 MPa, that is, the strength of the composites bipolar plates was improved significantly by adding CFs. The flexural strength of EG/CF filled CPCs had more complicated behavior and also higher values than that of EG/FG filled CPCs. The flexural strength initially increased and reached the highest value at the CF ratio of 24 wt%, and then decreased afterward. The flexural strength was already greater than 50 MPa at the CF ratio of 6 wt% and further increased up to 58 MPa at 24 wt%. Even the initial strength value of 52 MPa was higher than the optimized value of EG/FG filled CPCs. This behavior resulted from the strengthening effect of CFs. CFs located between compressed EGs bound them to each other in Fig. 12(a). Adding the excessive CF, however, generated voids among the fibers. As mentioned in the density analysis, these voids gave rise to stress concentration, so the flexural strength deteriorated over 30 wt%. This analysis could be supported by the analysis of the relative density. From these results, the range from 6 to 24 wt% is recommended for the proper CF ratio of EG/CF filled CPCs.

Results reveal that all specimens of various CF ratios effectively improve the flexural strength and could certainly achieve the commercial requirements, and the improvement level by using CFs is greater than that by using FG particles.

3.2.3. Electrical Conductivity

The electrical conductivity is a function of the conductive network among the conductive fillers. Even though CF is also a conductive material, the electrical contribution to the conductive network is much lower than EG, even than that of FG particles because of CF's needle-like shape. Figure 13(b) shows that the electrical

Table 3.

Optimal properties of CPCs according to the type of ancillary fillers

Conductive type	Weight ratio (wt%)	Flexural strength (MPa)	Electrical conductivity (S/cm)
EG/100 μm FG	15:60:25	51	390
EG/7 μm FG	7.5:67.5:25	50	130
EG/CF	36:24:40	58	290

conductivity decreased rapidly with increasing CF ratios. The electrical conductivity was initially 660 S/cm at the CF ratio of 6 wt%, and decreased continuously, dropping below the PEMFC specification at about 42 wt%.

The reasons for the decreasing tendency were considered to be the following. One was the reduction of the amount of EG, which is excellent in forming the conductive network by direct contact between particles. The other reason was the voids that occurred at the excessive fiber region and deteriorated the conductive network formed among EGs.

3.3. Comparison of Three Types of Tested CPCs

Table 3 is the results of the optimization of material properties for three different cases of CPCs with respect to the weight contents of fillers and resin. CPCs using 100 μm FG had the optimal flexural strength of 51 MPa and electrical conductivity of 390 S/cm at the FG ratio of 60 wt%, and CPCs using 7 μm FG had 130 S/cm and 50 MPa at the FG ratio of 67.5 wt%. While the flexural strengths were similar, the electrical conductivity of the case using 100 μm FG was about 3 times higher than that of the case using 7 μm FG because of the better electrical contribution. CPCs using CF had the highest flexural strength of 58 MPa, and a middle-level electrical conductivity of 290 S/cm at the CF ratio of 24 wt%. This shows that CFs were excellent in strengthening the mechanical property in the proper adding range (from 6 to 24 wt%) at which there were no voids. Overall, the optimal mechanical and electrical properties of all cases satisfied the commercial requirements and were good enough to be applied to the bipolar plate for PEM fuel cells.

4. Conclusions

This work focused on optimizing of the mechanical and electrical properties of EG filled hybrid CPCs prepared by a preform molding technique. Expanded graphite was excellent in forming the conductive network in CPCs but produced poor mechanical properties. The ancillary fillers, 100 μm FG, 7 μm FG and CF, were added to the composites to improve mechanical properties, especially flexural strength.

In the case of EG/FG filled CPCs, as the ratio of FG increased, the flexural strength increased because of the reduction of the intra-particle porosity in CPCs, especially in EG. On the other hand, the electrical conductivity decreased due to the

reduction of the absolute amount of EG, which is excellent in forming the conductive network. CPCs using 100 μm FG showed a high flexural strength at a FG ratio of 60 wt% while maintaining a high electrical conductivity. This was attributed to the superior level of densification in CPCs using 100 μm FG rather than 7 μm FG. In the case of EG/CF filled CPCs, meanwhile, the flexural strengths were greater than 50 MPa and had a maximum at 24 wt%. This behavior resulted from the interaction between the strengthening effect of fibers and the deteriorating effect of voids. The electrical conductivity decreased sharply with increasing CF ratio owing to not only the reduction of the amount of EG but also the increase of voids which deteriorated the conductive network.

The optimized properties for all kinds of CPCs achieved the commercial requirements, so they can be applied to the bipolar plate of PEM fuel cells. The principal properties of the materials, such as the electrical conductivity and flexural strength, kept pace with those of the previous research. Future work will focus on improving the mechanical properties and examining electrical conductivity in the through-plane direction, gas permeability, etc.

Acknowledgements

This study was supported by National RD and D Organization for Hydrogen and Fuel Cell and Ministry of Commerce, Industry and Energy, Korea.

References

1. K. Joon, Fuel cells — a 21st century power system, *J. Power Sources* **71**, 12–18 (1998).
2. K. Sopian and W. R. Wan Daud, Challenges and future developments in proton exchange membrane fuel cell, *Renew. Energy* **31**, 719–727 (2006).
3. M. A. J. Cropper, S. Geiger and D. M. Jollie, Fuel cells: a survey of current developments, *J. Power Sources* **131**, 57–61 (2004).
4. P. Zegers, Fuel cell commercialization: the key to a hydrogen economy, *J. Power Sources* **154**, 497–502 (2006).
5. D. Rastler, Opportunities and challenges for fuel cells in the evolving energy enterprise, *Fuel Cells Bull.* **3**, 7–11 (2000).
6. H.-C. Kuan, C.-C. M. Ma, K. H. Chen and S.-M. Chen, Preparation, electrical, mechanical and thermal properties of composite bipolar plate for a fuel cell, *J. Power Sources* **134**, 7–17 (2004).
7. A. Hermann, T. Chaudhuri and P. Spagnol, Bipolar plates for PEM fuel cells: a review, *Intl. J. Hydrog. Energy* **30**, 1297–1302 (2005).
8. E. Middelmann, W. Kout and B. Vogelaar, Bipolar plates for PEM fuel cells, *J. Power Sources* **118**, 44–46 (2003).
9. V. Mehta and J. S. Cooper, Review and analysis of PEM fuel cell design and manufacturing, *J. Power Sources* **114**, 32–53 (2003).
10. R. Blunk, F. Zhong and J. Owens, Automotive composite fuel cell bipolar plate: hydrogen permeation concerns, *J. Power Sources* **159**, 533–542 (2006).
11. S.-J. Lee, C.-H. Huang and Y.-P. Chen, Investigation of PVD coating on corrosion resistance of metallic bipolar plates in PEM fuel cell, *J. Mater. Process. Technol.* **140**, 688–693 (2003).

12. E. A. Cho, U.-S. Jeon, H. Y. Ha, S.-A. Hong and I.-H. Oh, Characteristics of composite bipolar plates for polymer electrolyte membrane fuel cells, *J. Power Sources* **125**, 178–182 (2004).
13. A. Kumar and R. G. Reddy, Materials and design development for bipolar end plates in fuel cells, *J. Power Sources* **129**, 62–67 (2004).
14. S. I. Heo, J. C. Yun, Y. C. Yang and K. S. Han, Fabrication process and characterization of conductive composite for PEFC bipolar plates, in: *Proc. 4th ACCM*, WP. Sydney, Australia, pp. 870–875 (2004).
15. H. Wolf and M. Willert-Porada, Electrically conductive LCP-carbon composite with low carbon content for bipolar plate application in polymer electrolyte membrane fuel cell, *J. Power Sources* **153**, 41–46 (2006).
16. S. H. Kim and H. T. Hahn, Size effect in particulate metal matrix composites: an analytical approach, *Adv. Compos. Mater.* **15**, 175–191 (2006).
17. M. Wissler, Graphite and carbon powders for electrochemical applications, *J. Power Sources* **156**, 142–150 (2006).
18. S. I. Heo, J. C. Yun, K. S. Oh and K. S. Han, Influence of particle size and shape on mechanical and electrical properties of graphite reinforced conductive polymer composites for the bipolar plate of PEM fuel cells, *Adv. Compos. Mater.* **15**, 115–126 (2006).
19. E. A. Cho, U.-S. Jeon, H. Y. Ha, S.-A. Hong and I.-H. Oh, Characteristics of composite bipolar plates for polymer electrolyte membrane fuel cells, *J. Power Sources* **125**, 178–182 (2004).
20. H. Tsuchiya and O. Kobayashi, Mass production cost of PEM fuel cell by learning curve, *Intl. J. Hydrog. Energy* **29**, 985–990 (2004).
21. X. Yan, M. Hou, H. Zhang, F. Jing, P. Ming and B. Yi, Performance of PEMFC stack using expanded graphite bipolar plates, *J. Power Sources* **160**, 1320–1328 (2006).
22. A. Heinzel, F. Mahlendorf, O. Niemzig and C. Kreuz, Injection moulded low cost bipolar plates for PEM fuel cells, *J. Power Sources* **131**, 35–40 (2004).
23. A. Müller, P. Kauranen, A. von Ganski and B. Hell, Injection moulding of graphite composite bipolar plates, *J. Power Sources* **154**, 467–471 (2006).
24. B. D. Cunningham, J. Huang and D. G. Baird, Development of fuel cell bipolar plates from graphite filled wet-lay thermoplastic composite materials, *J. Power Sources* **150**, 110–119 (2005).
25. B. D. Cunningham, J. Huang and D. G. Baird, Development of bipolar plates for fuel cells from graphite filled wet-lay material and a thermoplastic laminate skin layer, *J. Power Sources* **165**, 764–773 (2007).
26. S. I. Heo, K. S. Oh, J. C. Yun, S. H. Jung, Y. C. Yang and K. S. Han, Development of preform molding technique using expanded graphite for PEM fuel cell bipolar plates, *J. Power Sources* **171**, 396–403 (2007).
27. A. Kelly and C. Zweben, *Comprehensive Composite Materials. Polymer Matrix Composites*, vol. 2. Pergamon, UK (2000).
28. A. Celzard, J. F. Maréché and G. Furdin, Modelling of exfoliated graphite, *Prog. Mater. Sci.* **50**, 93–179 (2005).
29. A. Celzard, J. F. Maréché and G. Furdin, Surface area of compressed expanded graphite, *Carbon* **40**, 2713–2718 (2002).
30. A. L. Dicks, The role of carbon in fuel cells: review, *J. Power Sources* **156**, 128–141 (2006).
31. S. I. Heo, K. S. Oh, J. C. Yoon and K. S. Han, Electrical and mechanical properties of graphite particle/carbon fiber hybrid conductive polymer composites, *J. Korea Soc. Compos. Mater.* **19**, 7–12 (2006).